

FURTHER PROGRESS IN THE DEVELOPMENT OF THE MICROSTRIP GAS CHAMBER

F. Angelini, R. Bellazzini, A. Brez, E. Focardi, T. Lomtadze, M. M. Massai, G. Spandre and M. R. Torquati,
INFN and University of Pisa, via Livornese 582, 56010 S. Piero a Grado, Pisa, Italy

R. Bouclier, J. Gaudaen and F. Sauli.
CERN, Geneva, Switzerland

A. Perret.
CSEM, Neuchatel, Switzerland

We describe the operating principles of the microstrip gas chamber and the main results of measurements realized with several prototype devices in the detection of X-rays and charged particles. Detectors with 3, 5 and 10 μm anode widths and 125 or 200 μm pitch have been successfully tested. A gas gain of 10^4 and an energy resolution of 11% fwhm at 6 KeV have been measured. A localization accuracy for minimum ionizing particles of 30 μm rms, a two track resolution of 250 μm and a high rate capability (above $2 \cdot 10^7 \text{ cm}^{-2}\text{s}^{-1}$) make the device a good candidate for tracking at high luminosity colliders. Tests of survivability and of operation of the detector with fast gas mixtures have been performed.

1. STRUCTURE OF THE DETECTOR

The microstrip gas chamber was introduced some time ago in an attempt to reproduce the field structure of multiwire chambers, at a much smaller scale^{1,2}. It consists essentially in a sequence of alternating thin conductive anode and cathode strips placed on an insulating support; a drift electrode defines a region of collection of charges, and application of the appropriate potentials on anodes and cathodes create a proportional gas multiplication field.

Fig.1 shows the computed field lines in the multiplying region at typical values of the operating voltages³. One can understand the operation of the device as follows: drift lines connecting the upper cathode to the anode strips concentrate on the anodes, even more so due to the high potential difference between anode and cathode strips; the high electric field in the neighbourhoods of the anodes results in gas amplification. The major part (>70%, according to fig.1) of the positive ions created during the avalanche process, drift back to the close cathodes along the field lines, inducing signals on both anode and cathode strips.

For the measurements described in this report, we have used several detectors having cathode strips widths between 30 and 60 μm and anode strips between 3 and

10 μm , at a 200 μm pitch (see fig.2). A detector having a 125 μm anode pitch has been also successfully tested.

Three kinds of glass have been used as substrate differing mainly for their surface resistivity (10^{10} - $10^{13} \Omega/\square$). The surface resistivity affects the gain drift which is observed in the first minutes after voltage switch on. The lowest resistivity glass showed an overall gain drift of $\approx 8\%$.

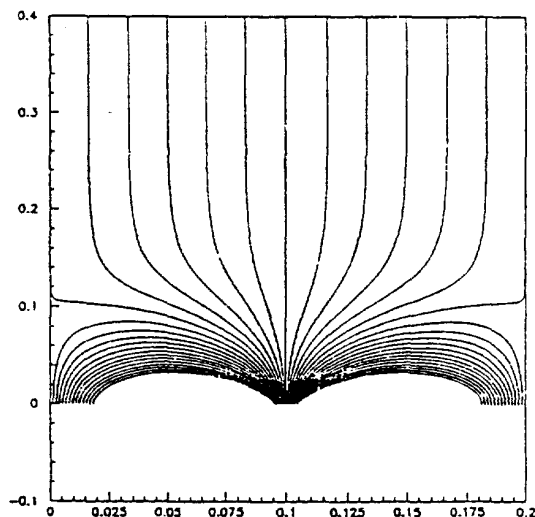


FIGURE 1
Field lines of one cell of the microstrip gas chamber.

The detectors are made using a microelectronics technology, namely electron beam lithography for the mask scribing and photolithography and thin film deposition to engrave $2\mu\text{m}$ thick aluminium strips onto a $500\mu\text{m}$ thick glass substrate. The intrinsic accuracy of this kind of technology is $0.1\mu\text{m}$. The active area of the devices was $80\times 80\text{mm}^2$, although only a limited number of strips were actually readout. A conductive electrode on the back plane slightly influences the operating gain; conveniently stripped, it can be used to obtain a second coordinate of the avalanche. Drift gaps between 2 and 6 mm were used in the detectors, the shorter gaps being favoured for detection of charged particles (since they imply a better time resolution).

In the case of cathode readout, all the anodes were connected together and to the (positive) high voltage, while the cathode strips were connected to the virtual ground of a low input impedance charge sensitive amplifier. In the case of anode readout, all the cathode strips were connected together and to the (negative) high voltage, while the anode strips were individually readout. In a new detector that is now under test, the anode strips are connected to high voltage through individual $2\text{M}\Omega$ current limiting resistors which are directly built on the substrate. This opens the possibility of having at the same time both anode and cathode readout. The double readout could improve substantially the position resolution.

2. GAS GAIN, ENERGY RESOLUTION AND RATE DEPENDENCE.

Fig.3 shows the gas gain as a function of anodic voltage obtained with a detector having a $5\mu\text{m}$ anode width and a $200\mu\text{m}$ pitch. The gas filling was Argon-Ethane (90-10). Proportional gas gain around 10^4 can be safely reached with several fillings 4,5 when working with detectors with 3, 5 or $10\mu\text{m}$ anode widths and $200\mu\text{m}$ pitch. The detector with a pitch of $125\mu\text{m}$ and a $5\mu\text{m}$ anode width had a proportional gain limited to 10^3 . For the same gas gain the operating voltages were correspondingly lower for the 3 and $5\mu\text{m}$ anode widths in comparison with the $10\mu\text{m}$ anode width (for example, 400 Volt versus 500 Volt anode cathode potential difference for 3 and $10\mu\text{m}$ widths respectively). The best energy resolution was obtained with the thinnest anode strip ($3\mu\text{m}$).

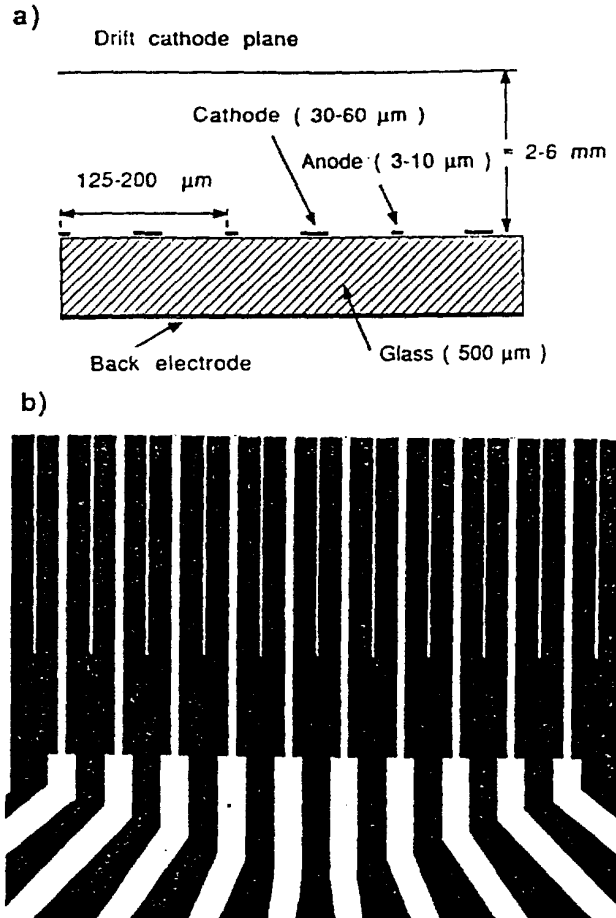


FIGURE 2

a) A cross section of the detector
b) A microphotograph of the anode-cathode structure and of the cathode fanout

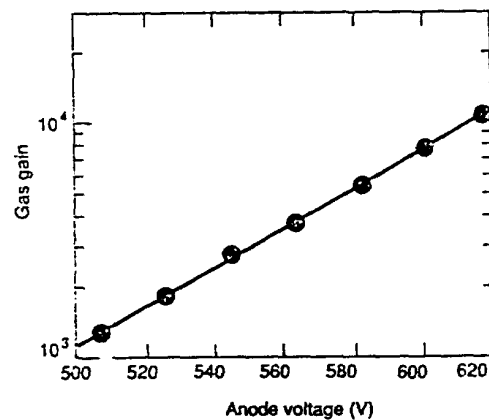


FIGURE 3

The gas gain as a function of anodic voltage

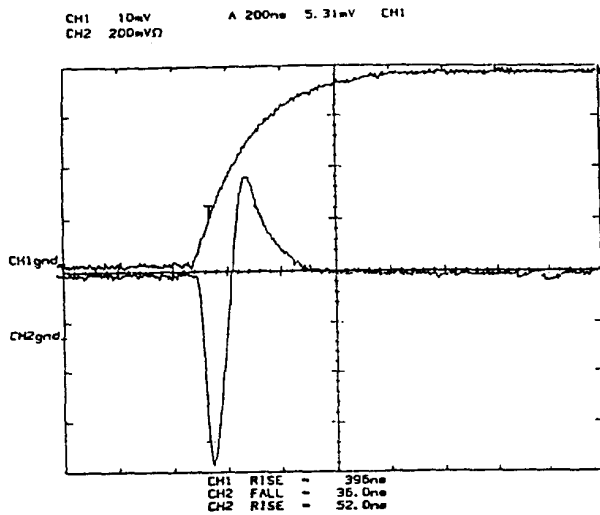


FIGURE 4
Upper trace: the charge signal (single shot) observed on a digital oscilloscope (differentiation time constant $\tau = 200 \mu\text{s}$)
Lower trace: the same signal after amplification and fast differentiation ($\tau = 30 \text{ ns}$).

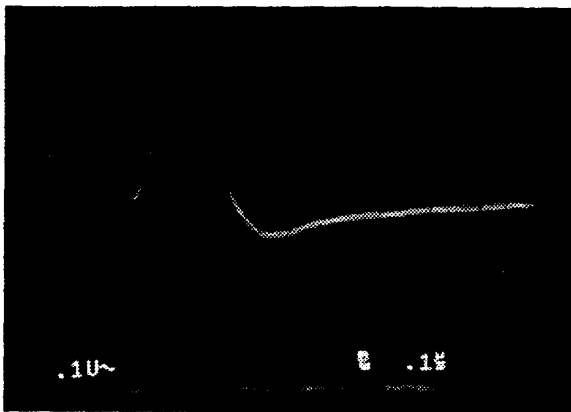


FIGURE 5
The anode signals with ^{55}Fe illumination.

The upper trace of fig.4 shows the charge signal (single shot) as a function of time observed on a digital oscilloscope ($200 \mu\text{s}$ differentiation time constant). The interesting feature is the fast collection time ($\approx 100 \text{ ns}$) of positive ions to the close cathodes which are only $60 \mu\text{m}$ apart in this case. The lower trace shows the same signal after amplification and fast differentiation ($\tau=30 \text{ ns}$). The signal to noise ratio is > 100 .

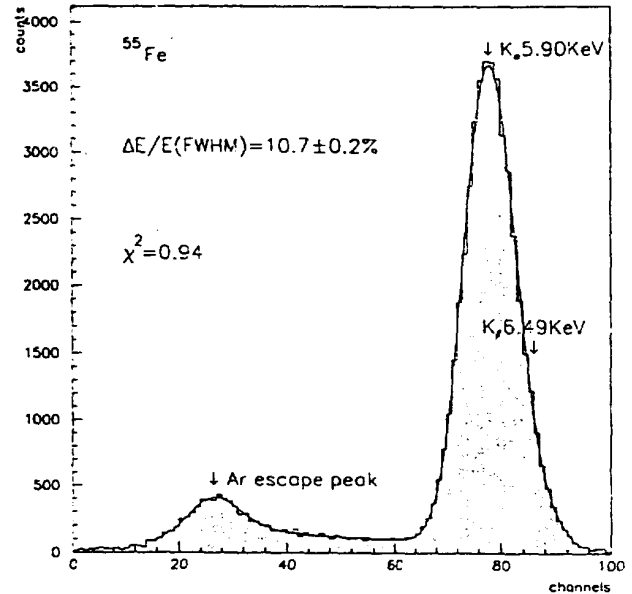


FIGURE 6
Pulse height spectrum of the ^{55}Fe signals shown in fig.5;
bin width = 56 eV , fwhm at $5.95 \text{ KeV} = 10.7 \pm 0.5\%$.

Fig.5 shows an analog oscilloscope picture of several pulses coming out of the detector with a $3 \mu\text{m}$ anode, working with an Argon-Ethane (90-10) gas mixture. The corresponding pulse height spectrum measured on a group of anode strips for 5.9 KeV x-rays is shown in fig.6; it is rather uniform over the sensitive area of the detector, with a fwhm of $10.7 \pm 0.5\%$. This resolution is remarkably good when compared to typical results obtained in multiwire proportional chambers and it is very close to the statistical limit for this gas mixture.

While a gas gain of 10^4 is probably high enough when the primary ionization is $> 100 e^-$, it could become a limiting factor when the primary ionization is quite lower as when using very thin detectors ($2 - 3 \text{ mm}$) at atmospheric pressure. Thin detectors are needed, for example, at the next high luminosity hadron colliders (LHC, SSC) to reduce the detector memory (i.e. the electron drift time). For tracking at LHC or SSC a higher gas gain could therefore be desirable. Because no more gain could be obtained from the amplification process around the thin anode strips, we have tried to get a further stage of gain from the drift region (5 mm thick) which is in

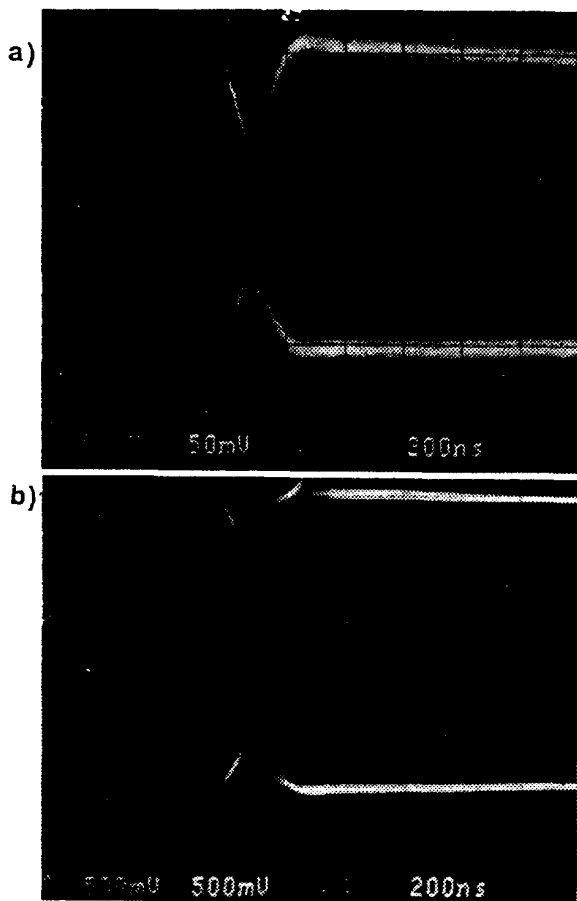


FIGURE 7

a) cathode (upper trace) and anode (lower trace) ^{55}Fe signals observed when the detector works without gas gain from the drift region;
 b) the same of a) but with a contribution to the gain coming also from the drift region.

front of the amplification region⁶. The electric field was originally set to 2 kV/cm which is below the threshold for gas multiplication in an Argon-DME mixture (90-10). By reducing the quencher fraction to 5 %, and by increasing the field to 6 kV/cm, we succeeded in starting the multiplication process already in the uniform field region. A 6 kV/cm field is rather modest and quite comfortable. Fig.7a) and fig.7b) show the ^{55}Fe signals obtained from the anodic and cathodic strips when operating the chamber in the two different regimes, i.e. with or without amplification in the drift region. When all the gain comes from the anodic strips (fig.7a) the signals show the

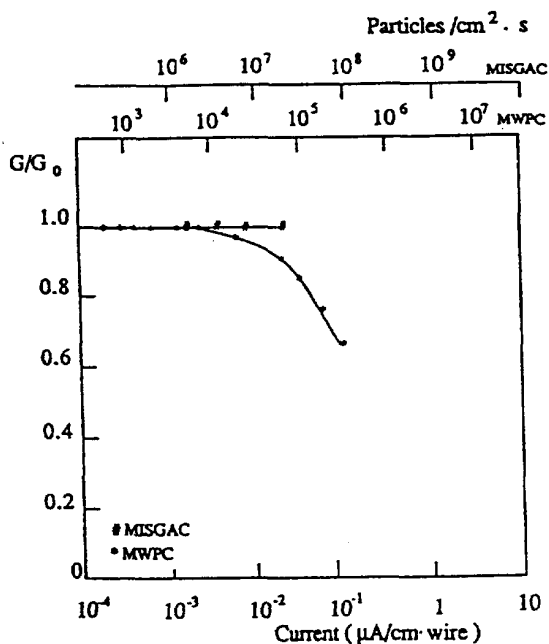


FIGURE 8

The relative gas gain versus the wire current and versus the incoming flux for a standard MWPC (*) and a microstrip gas chamber (#).

classical ^{55}Fe line (gain independent of the conversion point), while when working with two stages of gain the signals show an almost continuous spectrum typical of a parallel plate operation (gain dependent on the conversion point , $G(x) = e^{ax}$, where x is the drift path of the photoelectrons). Note the change of vertical scale of a factor 10. This regime has been used for the 125 μm anode pitch detector whose proportional gain was limited to 10^3 .

To check the rate dependence of the proportional gain, the chamber was exposed to an x-ray generator with controlled variable flux; the largest fraction of detected x-rays corresponds to the 8 KeV Cu line. At increasing values of the flux, the current, counting rate and pulse height spectrum were recorded on the cathode strips at fixed operating potentials. The result of the measurement is summarized in fig.8, providing the normalized gain as a function of the detector current per unit length of strip; a typical result obtained in a multiwire chamber is also shown for comparison⁷. As one can see, in the microstrip detector

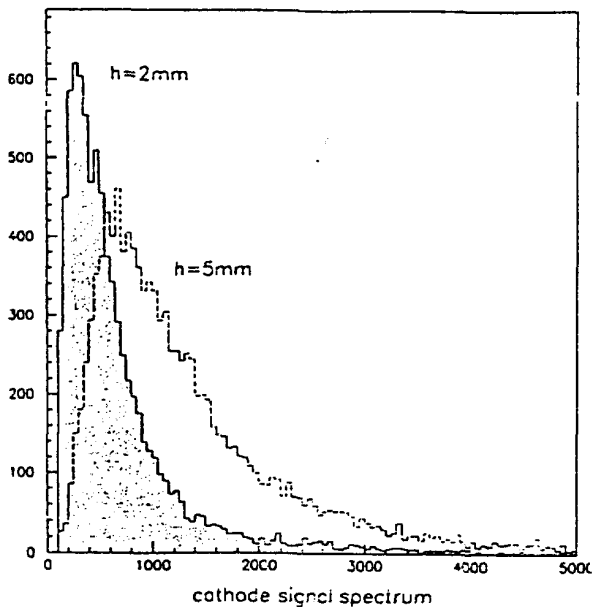


FIGURE 9
Pulse height spectrum of the sum of cathodic signals produced by minimum ionizing particles (Xe-DME) with 2 and 5 mm of drift gap.

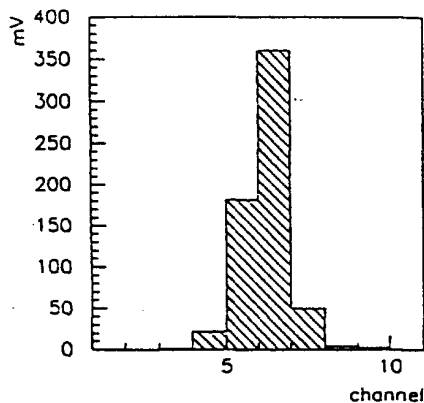


FIGURE 10
An example of cathode charge distribution

the gain is unchanged at currents an order of magnitude larger than in a MWPC; taking into account the reduction in pitch (at least by a factor of ten), one expects a rate capability in the microstrip chamber more than two orders of magnitude larger than in a MWPC, as shown by the upper scale in the figure. An actual measurement in a high intensity minimum ionizing particles beam has however still to be performed.

3. LOCALIZATION ACCURACY AND MULTITRACK RESOLUTION.

Localization in the direction perpendicular to the strips can be performed by recording the induced charge profile on the cathode strips and computing event per event the corresponding center of gravity. Preliminary measurements realized with a ^{55}Fe x-ray source indicated a localization accuracy in this case better than $80\mu\text{m}$ rms, limited by the collimator width ².

For a measurement of efficiency and localization accuracy for minimum ionization particles, a microstrip chamber was installed in a high energy test beam at CERN, using as reference the space coordinates provided by a pair of silicon strip detectors ⁸. For each event, the induced charge profile on 10 adjacent cathode strips was recorded, thus covering a 2 mm region; the gas filling for these measurements was Argon or Xenon with about 10% Dimethylether (DME) as quencher. Xenon was used in order to increase the energy loss and reduce their primary ionization fluctuations in the thin (5 mm thick) drift gap constituting the sensitive volume of the detector.

Fig.9 shows an example of pulse height spectrum for the Xe-DME mixture, integrated over the cathode strips, and fig.10 a typical induced charge profile for a single track. A scatter plot of the coordinate measured in the gas microstrip chamber, as a function of the position provided by the silicon strip detectors, is shown in fig.11 : it shows a good linearity and a dispersion of about $40\mu\text{m}$ rms; this is better seen in the projected histogram of fig.12. Taking into account the estimated dispersion of the silicon strip detectors, one can infer an intrinsic localization accuracy for the microstrip gas chamber of around $30\mu\text{m}$ rms. The measurements in Ar-DME provide, as expected, a slightly worse space resolution.

The multitrack resolution depends on the rms of the induced charge profile. Fig.13 shows this quantity measured for minimum ionizing particles in Xe-DME. It has an average value of $125\mu\text{m}$; assuming that two tracks can be resolved if the corresponding induced pulse profiles are at least two standard deviations apart, we infer a multitrack resolution of $250\mu\text{m}$.

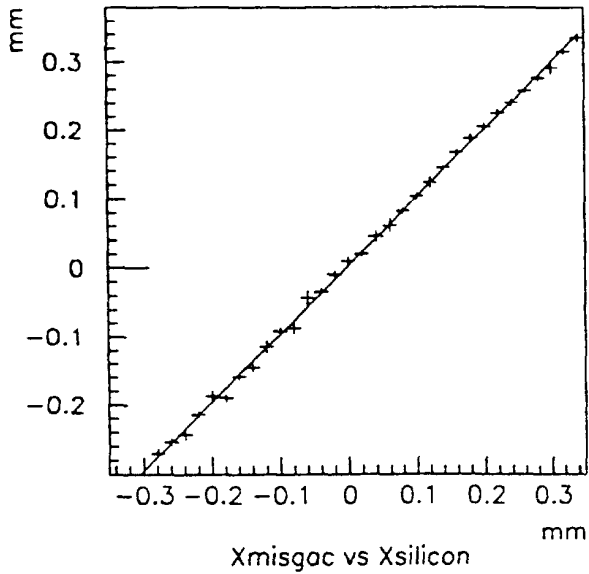


FIGURE 11

The correlation between the coordinates measured by the silicon detectors and the microstrip gas chamber.

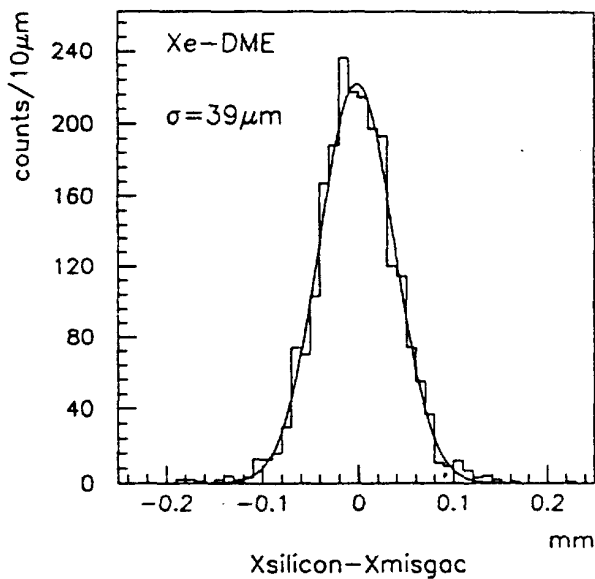


FIGURE 12

Distribution of the differences between the coordinates measured with the silicon detectors and the microstrip gas chamber.

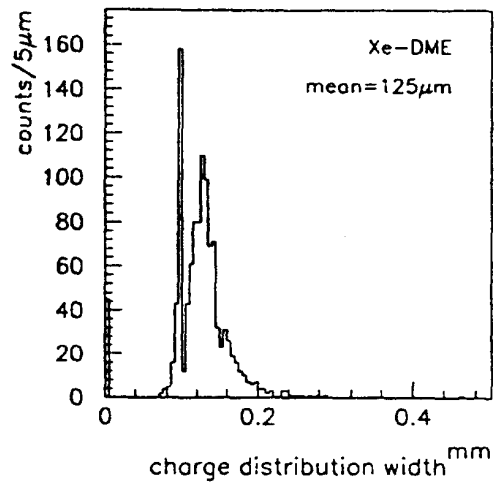


FIGURE 13

The width (rms) of the charge distribution

4. OPERATION OF THE DETECTOR WITH CF_4 BASED GAS MIXTURES..

Any detector aiming to work at SSC or LHC has to be fast to reduce the memory time and therefore the cell occupancy. Fast, in this case, means that the charge collection time which defines the pulse leading edge, has to be in the few ns range to be comparable with the bunch crossing separation. Standard, Argon based, gas mixtures are relatively slow ($v_{\text{drift}}=20$ ns/mm) and the gas thickness has to be large because of the low ionization density of Argon (≈ 20 clusters/cm). CF_4 is a very fast ($v_{\text{drift}}=10$ ns/mm), very dense (≈ 50 clusters/cm) new gas recently proposed for gas detectors. Furthermore it seems to have etching properties of the polymerization products which are at the origin of the ageing process.

We have successfully operate a 2 mm thick microstrip gas chamber with a CF_4 (80)-Isobutane(20) gas mixture. Fig.14 shows the average pulse observed on a single strip with a ^{90}Sr β source. It is a very fast pulse (13 ns rise-time) having a total duration of ≈ 50 ns. This is a suitable pulse for a tracker at the high luminosity hadron colliders ($\leq 1\%$ occupancy at 20 cm from the LHC beam axis). Fig.15 shows the pulse height spectrum of the anode OR observed when illuminating the detector with a ^{90}Sr source. The acquisition was triggered by a central cathode strip to be sure that the β ray is within the detector active region. The spectrum is completely apart from the pedestal distribution (left peak).

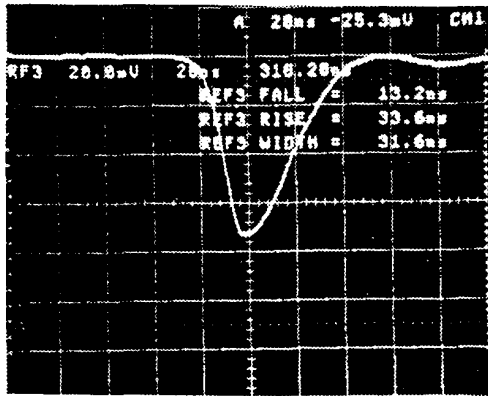


FIGURE 14

Average pulse from a single strip with a ^{90}Sr β source, observed on a digital oscilloscope.

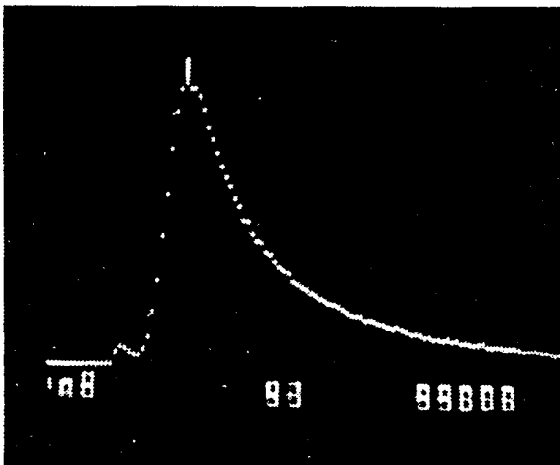


FIGURE 15

Pulse height spectrum of the anode OR with a ^{90}Sr β source.

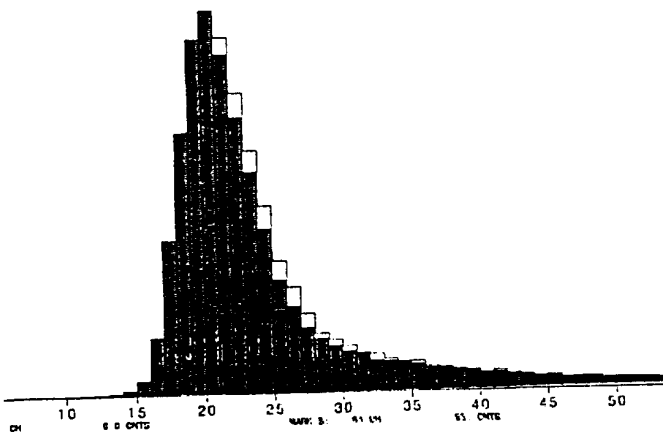


FIGURE 16

Landau distributions measured in two 100 ms time windows at the beginning and at the end of the spill of the NA-34 (Helios) intense proton beam at CERN.

5. TEST OF SURVIVABILITY OF THE DETECTOR IN A HIGH-RATE ENVIRONMENT.

The test beam studies were performed with a low rate charged particle beam (10 KHz). To study the survivability of the detector in the much more severe experimental and environmental conditions expected at the SSC or LHC, we moved the detector in the most intense beam existing today at CERN, which is the NA-34 (Helios) proton beam. This beam has, at focus, a flux of $\approx 10^7$ protons/mm².s. We placed the detector a few meters out of focus where the flux is reduced to $\approx 10^6$ protons/mm².s, which is very close to the most stringent requirement at LHC. We left the detector in the beam for three weeks, monitoring the Landau distribution from the OR of anode strips (gas filling Ar 80-Methane 20). No significant change was observed during this period. The integrated fluence was $\approx 10^{12}$ particles/cm². To study if there is any substrate charging at this very high rate, the Landau distribution was taken also in two different 100 ms time windows, one at the beginning of the beam spill and the second at the end of the spill. The spill duration was 2.4 s. No noticeable difference between the two distributions was observed (see fig.16), indicating that no charging process occurred at this rate.

6. CONCLUSIONS.

The microstrip gas chamber has been shown to allow fast and accurate detection of both soft x-rays and minimum ionizing particles. Its performances compare rather well to those obtained with solid state microstrip detectors; the advantages seem to be however a higher radiation resistance, a lower cost and a larger signal/noise ratio, this last point rather interesting in that it could lead to the use of cheaper and/or faster electronics readout.

Work is in progress to improve the operating characteristics of the device, the angular dependence of the localization accuracy and to study its long term stability. Use of small gaps and fast gases has been studied to take full advantage of the rate capability of the detector.

ACKNOWLEDGMENTS

We would like to thank C. Magazzù and G.C. De Carolis for the technical assistance.

REFERENCES

1. A.Oed et al. Nucl.Instr. and Meth A263 (1988) 351
2. F.Angelini et al., Nucl. Instr. and Meth. A283 (1989) 755.
3. P.Astier, Private communication.
4. F.Angelini et al. Particle World vol 1., n.3 (1990) 85
5. H.Hartjes et F.Udo, Proceedings of ECFA study week on Instr. Tech. for High-Luminosity Hadron Colliders, Barcelona (1989), CERN 89-10, 455.
6. F.Angelini et al., A microstrip gas avalanche chamber with two stages of gas amplification, to be published on Nucl. Instr. and Meth.
7. F.Angelini et al., Proceedings of ECFA study week on Instr. Tech. for High-Luminosity Hadron Colliders, Barcelona (1989), CERN 89-10, 465.
8. F.Angelini et al., Proceedings of the 1989 IEEE Symposium on Nuclear Science, San Francisco, January 1990.